Journal of Materials and Environmental Sciences
ISSN : 2028-2508
CODEN : JMESCN

J. Mater. Environ. Sci., 2018, Volume 9, Issue 4, Page 1247-1254

https://doi.org/10.26872/jmes.2017.9.4.136

http://www.jmaterenvironsci.com

Growth and characterization of electrodeposited orthorhombic $FePO_4.2H_2O$ material

H. Ould Bouamer[1],M. EL Joumani[1], M. Lakhal[1], G.Kaichouh[1], K. Ouzaouit[2], H. Faqir[2], A. EL Hourch[1], A. Guessous[1]*

[1]*Materials, Nanotechnologies and Environment Laboratory, Department of Chemistry, Faculty of Science Mohammed V University in Rabat, Morocco*

[2]*REMINEX Research Center - MANAGEM Group, Site de Hajar, BP 469 Marrakech, Morocco*

Received 17 Jan 2017,
Revised 27 Nov 2017,
Accepted 30 Nov 2017

Keywords

- ✓ Voltammetry;
- ✓ iron;
- ✓ deposit ;
- ✓ diffusion;
- ✓ $FePO_4 \cdot 2H_2O$

guessous95@yahoo.fr
Phone: +212661493849

Abstract

Orthorhombic hydrated phosphates $FePO_4 \cdot 2H_2O$ form has been synthesized by using the electrochemical oxidation of a solution containing a precursor of iron in phosphoric acid. By means of the voltammetry cyclic, we were able to show the mechanism of the formation of the electrolytic deposit by diffusion process. The study of the influence of certain parameters such as the concentration of iron ions, phosphoric acid H_3PO_4 and the scanning rates was realized in this article. A series of experiments including an X-ray diffraction study, thermogravimetric analysis and transmission electron microscopy investigation helped in determining the exact chemical formula of the obtained phase, i.e. $FePO_4 \cdot 2H_2O$. The phase exhibits an orthorhombic structure with **a=9.904Å; b=10.116Å; c=8.767Å.**

1. Introduction

Different types of iron phosphate are reported in the literature as monoclinic and trigonal $FePO_4$ [1-2] and $FePO_4$ hydrated phases, which include monoclinic and orthorhombic forms of $FePO_4 \cdot 2H_2O$ [1,3]. Iron phosphates exhibit different types of structures depending on the synthesis conditions. For example, $FePO_4$ shows a trigonal structure at normal pressure, but it converts to an orthorhombic structure at high-pressure [1]. Iron phosphates have been explored as cathode and anode materials [4-6]. Dongyeon Son and al. [4] report the superior electrochemical properties of iron phosphates as anode materials for lithium ion batteries with 375 mAh/g as capacity, while Yuesheng Wang and al [6] demonstrates for the first time that $FePO_4 \cdot 2H_2O$ can be used as the anode for an aqueous sodium ion battery. The capacity obtained in this case is of the order of 80 mAh / g at a rate of 0.5 C in a three-electrode system. $FePO_4.2H_2O$ material is also study as a promising precursor for the synthesis of $LiFePO_4$ [7-10] or as catalyst [11-12]and environment purification [13].

The synthesis of iron phosphate-based materials includes various types of preparation methods such as sol-gel[14], ion exchange [15], co-precipitation [16-17] and microwave-assisted synthesis [18]. The main disadvantages of these methods are a low production yield and complicated synthesis steps. It is why the development of a simple and cheap road of synthesis of iron phosphate-based material is of great interest.

The paper reports on a new and original way to prepare orthorhombic $FePO_4$ hydrated thin film by using the electrochemical oxidation of iron sulfate in H_3PO_4 solution at low temperature. Such a way was expected to produce films with fine particles owing to the intimate mixing of the component elements in the solution[19-21]. The synthesis of the orthorhombic $FePO_4$ hydrated thin film; the experimental conditions to obtain a pure phase and the characterization of the deposited films are described in the paper.

2. Materials and methods

All electrochemical experiments were carried out using a conventional set up comprising a three-electrode electrochemical cell connected to a computer-controlled Radiometer Analytical PGZ 301 potentiostat-galvanostat. The three-electrode electrochemical cell was placed in a double jacket to maintain a constant temperature throughout the experiment by circulation of thermo-stated water, i.e. 25°C or 70°C. The working electrode was a 2 cm^2 Platinium plate. A saturated calomel electrode (SCE) was used as the reference electrode

and the counter electrode was a wide-area Pt grid. The electrodes were placed in solutions comprising of ($FeSO_4.7H_2O$) in phosphoric acid (H_3PO_4).
Just prior to the deposition, the working electrode were polished using different grades of Al_2O_3 powder. The electrodes were rinsed with ultrapure water (18 MΩ.cm^{-1}). The solution was stirred throughout the experiment. The applied voltage is greater than 0.3V/SCE. White deposits resulting from the electrochemical oxidation of Fe^{2+} to Fe^{3+} were collected at the working electrode, washed with distilled water and then dried for several hours in air.Thermogravimetric analyses were carried out in air with a heating rate of 10 C/min using a TGA Q500 thermogravimetric analyzer. X-ray diffraction patterns were obtained with a X'Pert PRO diffractometer using Cu K_α radiation (λ=1.5406 Å) with operating voltage of 35 kV and a beam current of 30 mA. Infrared spectroscopy spectra were measured in KBr disks using a VERTEX 70 (IR/FT) instrument.

3. Results and discussion

3.1 Voltammogram of a solution of $FeSO_4.7H_2O$ in phosphoric acid

Figure 1 presents the voltammograms obtained at 25°C in a solution of Phosphoric acid in the presence and in the absence of $FeSO_4.7H_2O$at a scan rate of 100 mV/s. The applied voltage was varied from-0.3 V/SCE to 1 V/SCE. The figure 1 (1) concerns the electrolytic solution of solvent H_3PO_4 (1M), no peak was observed. Figure 1 (2) concerns the iron sulfate solution (0.2 M) in phosphoric medium (1M). In this case the currents density increase which is consistent with continuous oxidation of Fe^{2+} to Fe^{3+} onto the Platinum electrode. The reaction, which account for this oxidation is proposed as follows:

$$Fe^{2+} \rightarrow \quad Fe^{3+} + 1e^-$$

The current observed for anodic peak at ~0.3V/SCE. The cathodic peak at -0.002V/SCE during the reverse scan revealed the reduction of Fe^{3+} species formed during oxidation.

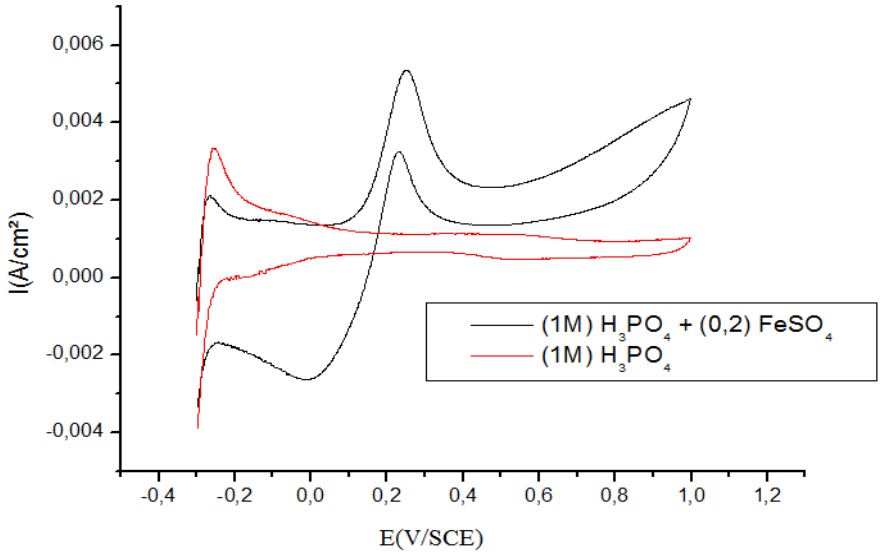

Figure 1: *Voltammograms recorded at 25°C a scan rate of 100 mV s^{-1} of different solution: ---- H_3PO_4 (1M) +Fe^{2+} (0.2M),----H_3PO_4 (1M)*

3.2. Influence of the concentration of H_3PO_4 solutions

Various H_3PO_4 concentrated solutions, from 1M to 5M were used for voltammetry experiments. Figure 2 shows the curves obtained for a $FeSO_4.7H_2O$(0.2 M) in these solutions. We notice that the current intensity increases with H_3PO_4 concentration. For concentrations above 2M of phosphoric acid no deposit is observed on the electrode. For the concentration of 1M of phosphoric acid, a crystallized deposit is obtained. For 2M of phosphoric acid the deposit is amorphous. The reactions, which account for this oxidation, are proposed as follows [22]:

$$Fe^{2+} \rightarrow \quad Fe^{3+} + 1e^-$$
$$Fe^{3+} + H_2O \rightarrow Fe(OH)^{2+} + H^+$$
$$Fe(OH)^{2+} + H_2O \rightarrow Fe(OH)^{+}_2 + H^+$$
$$Fe^{3+} + H_3PO_4 \rightarrow FeH_2PO_4^{2+} + H^+$$
$$FeH_2P\,O_4^{2+} + H_3PO_4 \rightarrow Fe(H_2PO_4)_2^{+} + H^+$$
$$Fe(OH)^{+}_2 + Fe(H_2PO_4)_2^{+} + 2H_2O \rightarrow 2(FePO_4 \cdot 2H_2O) + 2H^+$$

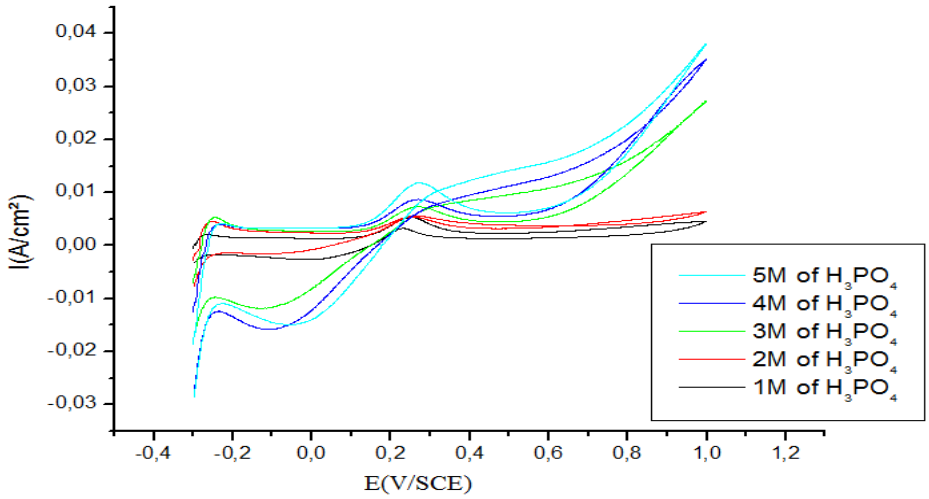

Figure 2:*Current-potential polarization curves of the $FeSO_4.7H_2O$in H_3PO_4 solutions. Scan rate=100 mV.s^{-1}*

We conclude that the presence of the entities $Fe(OH)^{2+}$; $Fe(OH)^{+}_{2;}$ $FeH_2PO_4^{2+}$; $Fe(H_2PO_4)_2^{+}$is necessary for the formation of the deposit[22].The latter are in very small quantity for concentrations greater than 2M in phosphoric acid, hence the absence of deposition at the surface of the electrode.On the other hand, in 1M and 2M, a deposit is observed on the surface of the electrode.

This work shows that the presence and the nature of the deposit onto the Platinum electrode is influenced by the ferrous sulfate concentrations and the phosphate concentrationswhen the voltage exceeded 0.3 V/SCE.

The anodic and cathodic peak current densities and ΔEp at different concentrated of H_3PO_4 are reported in table 1, we notice that ΔEp is in a potentially higher range than [59 mV]. The oxidation reaction of iron II to iron III is not reversible in this phosphoric acid concentration range.

The 1M concentration of phosphoric acid is chosen for the remainder of this work because it is the only concentration which has given rise to a crystallized deposit on the surface of the electrode.

Table 1: *Peak currents and peak potentials at different scan of 0.2M $FeSO_4.7H_2O$*

H_3PO_4 concentrated	I_{Pa} (A/cm²) (10^3)	I_{pc} (A/cm²) (10^3)	E_{pa} (V/SCE)	E_{pc} (V/SCE)	ΔEp(V)
1M	5.348	-2.642	0.250	-0.002	0.252
2M	6.753	-3.723	0.263	-0.124	0.387
3M	7.338	-12.05	0.269	-0.125	0.394
4M	8.690	-16	0.273	-0.114	0.387
5M	10.91	-15.56	0.276	-0.062	0.338

3.3. Influence of the concentration of $FeSO_4.7H_2O$ inphosphoric acid (1M)

Various $FeSO_4.7H_2O$concentration solutions, from 0.05 M to 0.2 M in phosphoric acid (1M), were used for voltammetry experiments. Figure 3 shows the voltammogram curve obtained in these solutions at 0.1 V.s^{-1}. The density of the anodic peak current increase with increasing $FeSO_4.7H_2O$ concentrations. Showing that the oxidation peak corresponds well to the oxidation of Fe^{2+} to Fe^{3+} at the working electrode, a thicker deposit is obtained for the concentration of 0.2 $FeSO_4.7H_2O$.This concentration was chosen for the rest of our experiments.

3.4 Influence of different potential scan rates.

Various scanning rates from 20 mV/s to 400 mV/s, were used for voltammetry experiments. Figure 4 shows the voltammogram curve obtained in these solutions. Current density of the anodic peak increases with increasing the scanning rates. The anodic and cathodic peak current densities at different potential scan rates are reported in table 2. We note that with the increasing of scan rate both anodic and cathodic peak current increases and the cathodic peak potentials have shifted towards negative values, while anodic peak potential move slightly towards more positive values. The peak potential separation, ΔEp = Epa- Epc is between 155-425 mV. It is increased with the variation of scan rate (Fig. 5). The ratio of the oxidation peak current to its corresponding reduction counterpart, I_{pa}/I_{pc} is about 2. These suggest that the redox process is quasi-reversible reaction rather than a reversible reaction.

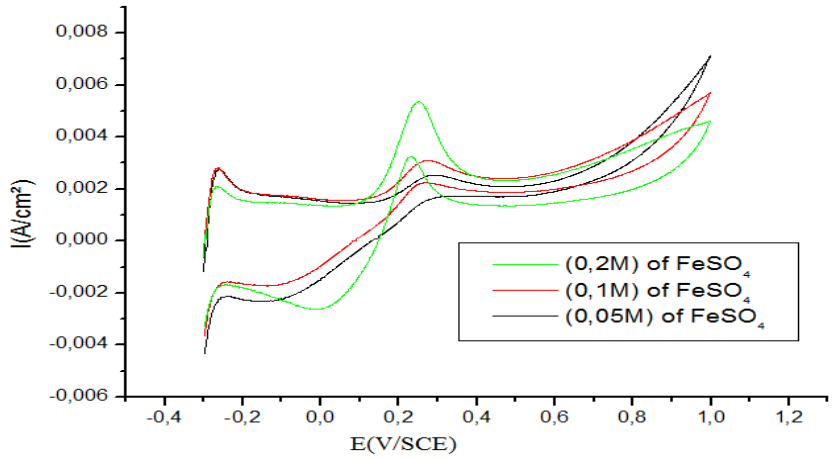

Figure 3*: Cyclic voltammograms for different concentrations of $FeSO_4.7H_2O$ in (1M) H_3PO_4 at a scan rate of 100 mV.s^{-1}*

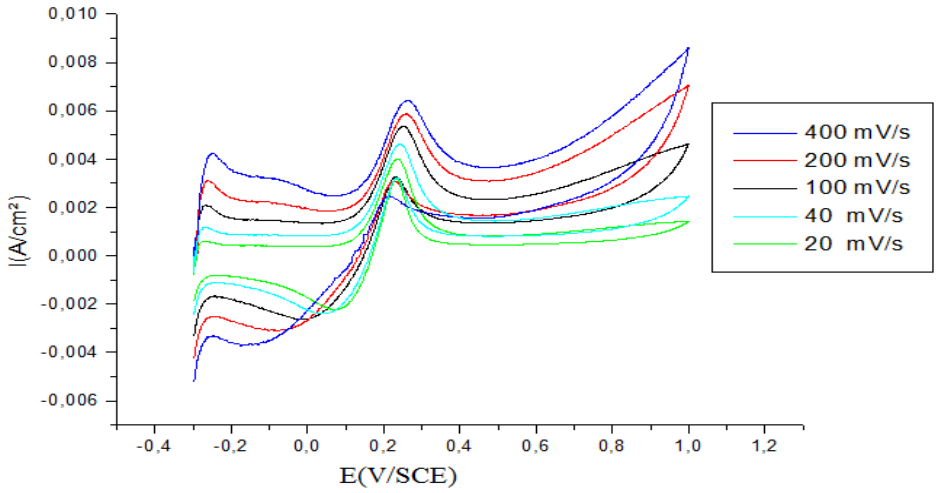

Figure 4: *Cyclic voltammograms for 0.2 M of $FeSO_4.7H_2O$ in phosphoric acid H_3PO_4 (1M), at different scan rates.*

Table 2: *anodic and cathodic peak current densities (ip) at different potential scan rates.*

v(V/s)	$v^{1/2}$ $(V/s)^{1/2}$	I_{pa}(A/cm²) 10^3	I_{pc}(A/cm²) 10^3	E_{pa}(V/SCE)	E_{pc}(V/SCE)	ΔEp(V)	I_{pa}/ I_{pc}
0.02	0.141	4.004	-2.24	0.235	0.069	0.155	1.78
0.04	0.2	4.608	-2.426	0.242	0.039	0.201	1.89
0.1	0.316	5.348	-2.642	0.250	0.002	0.252	2.02
0.2	0.447	5.884	-3.123	0.258	-0.075	0.340	1,88
0.4	0.632	6.445	-3.683	0.265	-0.153	0.425	1,74

In Fig. 6, it is apparent that the peak current for the electrochemical oxidation of Fe (II) in phosphoric 1M has linear relation with square root of scan rates. This observation is in favor of the fact that the electrode process is diffusion controlled with no adsorption on the electrode surface. As the Fe^{3+}/Fe^{2+} reaction is quasi reversible, the peak current Ip is given as follows [23]:

$$Ip = 0{,}4958 \times nFA\ (\alpha nF/RT)^{1/2} \times A \times D^{1/2} \times C \times v^{1/2} \qquad \text{Eqn.(1)}$$

The numerical constant corresponds to expressing I_p is the peak current (A); A is the surface area of the electrode (cm^2); D is the diffusion coefficient of the iron ion ($cm^2.s^{-1}$); C is the concentration of iron ($mol.cm^{-3}$); v is the scanning rate ($V.s^{-1}$); n is the number of electrons transferred in the electrode reaction. In this paper, n is equal to 1 and α is the coefficient of charge transfer. When the test temperature is kept at 25 ℃ the Eqn.(1) reduces to:

$$I_p = 2.99 \times 10^5 x\ n\ (\alpha n)^{1/2} AC\ D^{1/2}\ v^{1/2} \qquad \text{Eqn.(2)}$$

Assuming αn equal to 0.5[23,24], the diffusion coefficient of Fe^{2+} calculated from the slope of this straight line is $3{,}35 \times 10^{-9}$ $cm^2.s^{-1}$.The value of the diffusion coefficient calculated in phosphoric medium (1M) is lower than the value reported for Pt polished electrodes in aqueous medium $D_{Fe2+} = 5.4 .10^{-6}$ cm^2 s^{-1} [25]. This difference can be explained by the nature of the electrolyte used which is less conductive.

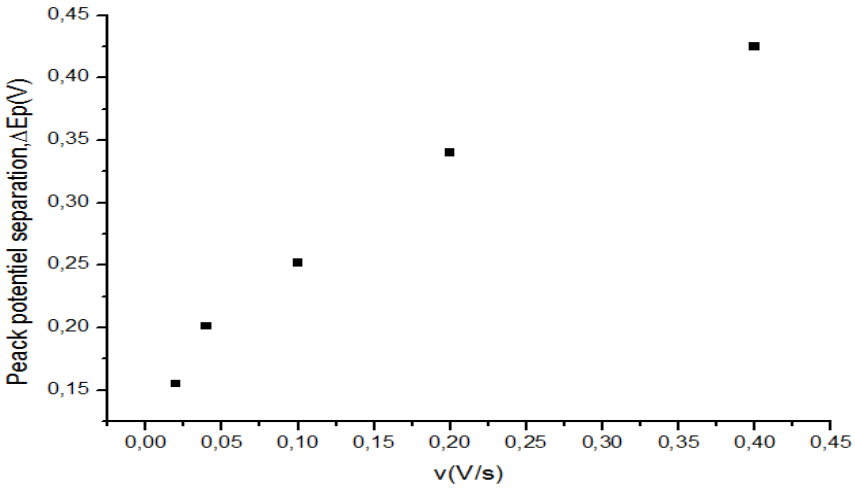

Figure 5 : *Variation of peak potential separation with scan rate of 0.2 M of $FeSO_4.7H_2O$ in phosphoric acid H_3PO_4 (1M)*

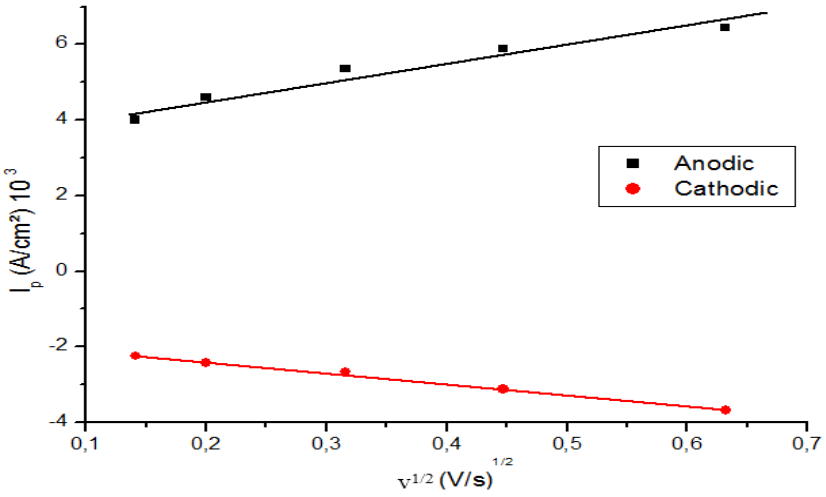

Figure 6*: anodic and cathodic peaks current densitys (i_{pa}) vs.$v^{1/2}$ for 0.2 M $FeSO_4.7H_2O$in 1M H_3PO_4*

3.5 Structure and morphology

On the basis of the above data, it appeared that deposits onto the Pt electrode could be obtained for E > 0.3V/SCEand for solutions 1M in phosphoric acid. Various deposits from solutions at 1M were then carried out by maintaining the oxidation potential E >0.3V/SCE at a constant value during several hours at 60°C. A SEM image of the white deposit obtained for a solution at H_3PO_4 (1M), $FeSO_4.7H_2O$ (0.2M), T= 60°C is shown in figure 7.

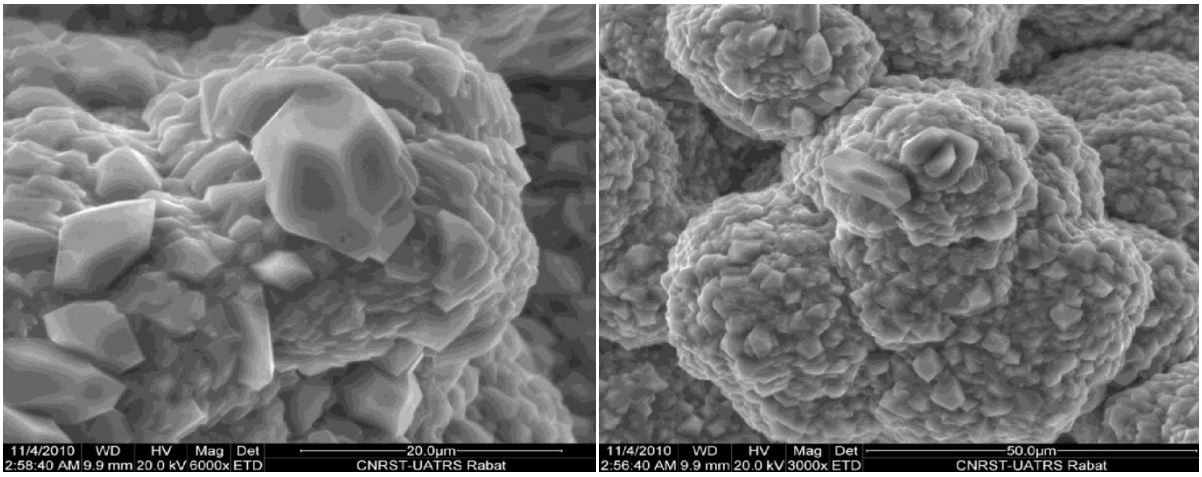

Figure 7: *SEM images of the white deposit obtained at 60C° after 7h of oxidation of Fe^{2+} (with various magnifications)*

The particles have the same dimension and the deposit is homogeneous. The high crystallinity is observed. A study by energy dispersive spectroscopy was carried out and helped in confirming the presence of Fe, O and P in the deposits. The ratio with the Fe/P of 1 indicted by EDAX analysis in figure 8, points clearly toward the

$FePO_4$ phase deposited onto the Pt electrode. However the accuracy of the data was not sufficient to allow obtaining an accurate chemical composition.

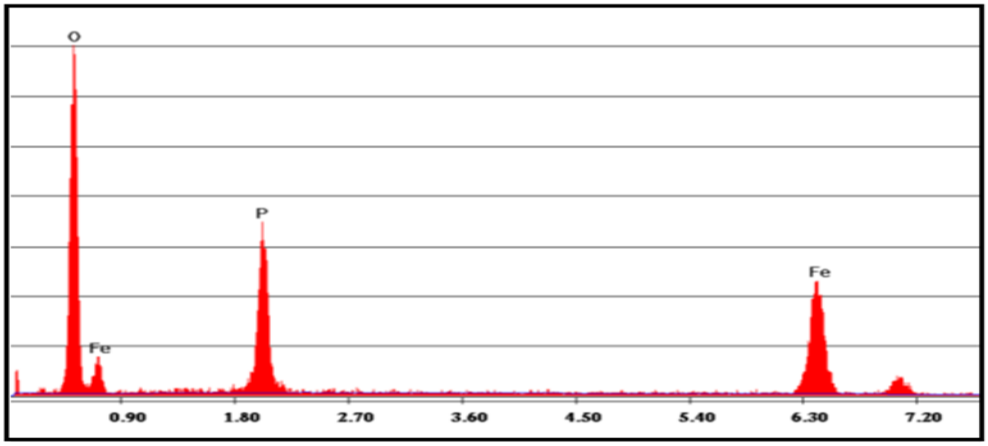

Figure 8: *EDX spectrum $FePO_4$, $2H_2O$*

The XRD pattern of the as-prepared deposit and the pics of PDF card 33-0667 are shown in Figure 9. All the diffraction peaks in pattern are in agreement with those of orthorhombic FePO4 $2H_2O$ (PDF card 33-0667).The strong and narrow diffraction peaks, indicate that the material is well crystallized.

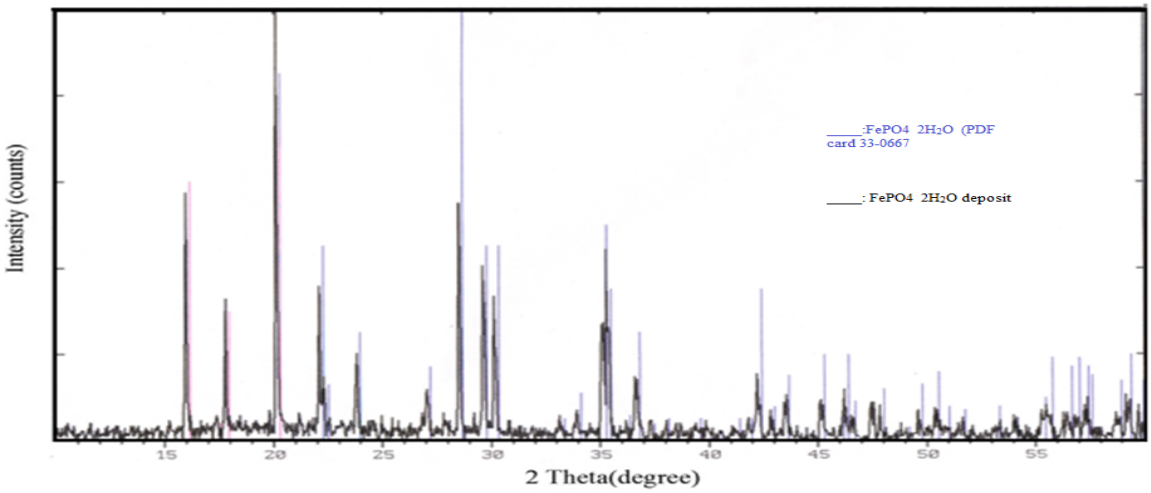

Figure 9: *XRD pattern of the as-prepared $FePO_4.2H_2O$.*

The XRD patterns were indexed with single-phase orthorhombic $FePO_4.2H_2O$. Without any impurities phase. The lattice parameters refined in the orthorhombic system are: a=9.904 Å; b=10.116 Å and c=8.767Å. Iron phosphate, FePO4 hydrated and not exist with different crystalline forms, as shown in Table 3. The parameters calculated for our deposit are in accordance with those obtained by [1].

Table 3: *Crystallographic parameters theoretical and calculated of orthorhombic $FePO_4$. $2H_2O$*

	Compound	**Space group**	**Crystallographic parameters**				**Reference**
			a (Å)	b (Å)	c (Å)	β (°)	
Theorical	α-$FePO_4$ quartz	P321	5.033	5.033	11.247	–	[2]
	Heterosite $FePO_4$	Pnma	9.814	5.789	4.782	–	[7]
	Monoclinic $FePO_4$	P21/n	5.307	9.754	8.675	90.16	[1]
	Monoclinic $FePO_4{\cdot}2H_2O$	P21/n	5.312	9.765	8.683	90.44	[3]
	Orthorhombic $FePO_4{\cdot}2H_2O$	Pbca	9,886	10,122	8.723	–	[1]
	$Fe_4(P_2O_7)_3$	Pbnm	9.562	21.509	7.545	–	[26]
Calculated (orthorombique)	Orthorhombic $FePO_4{\cdot}2H_2O$	Pbca	9,904	10,116	8,767		This Work

Several complementary techniques were used in order to confirm the obtained phases. The TG/DSC curves of $FePO_4.2H_2O$ are shown in Figure 10. From TG–DSC curves, the mass of the product decreased up to change after 195°C, with a total mass lost of 19.69 %, which is consistent with the theoretical content of the crystalline water molecules in $FePO_4$, $2H_2O$. From TG and DSC, the iron phosphate obtained by electrochemical method loses two water molecules at around 160 C°. Similar molecule loss has been observed, at higher temperature in [22, 27].

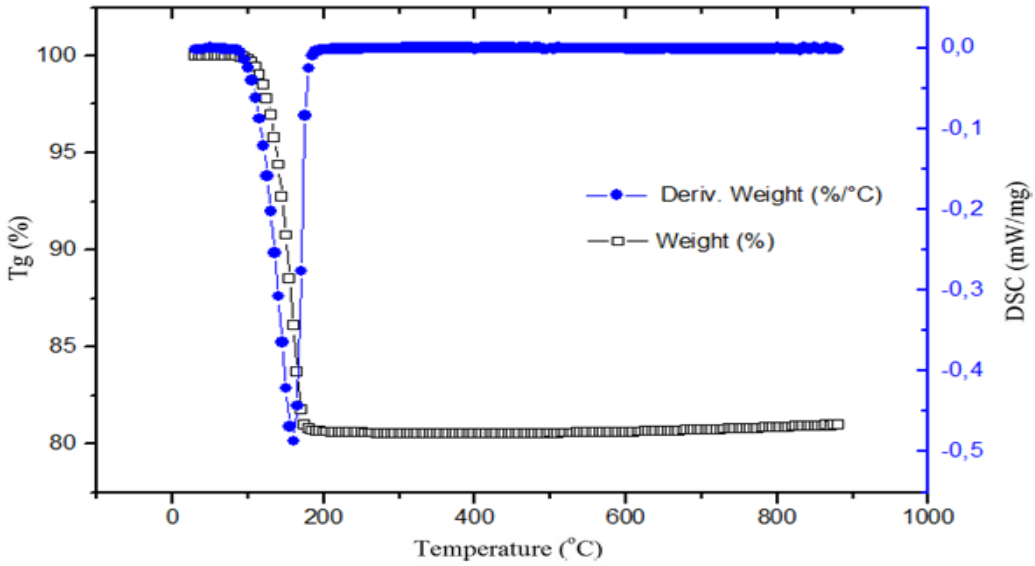

Figure10: *TGA and DSC of deposits obtained for solutions comprising 0.2 Mof $FeSO_4.7H_2O$ in phosphoric acid ($H_3PO_4$1M)*

Infrared spectrum(IR) of the material deposited is shown in Figure 11. The observed bands IR are in agreement with the conclusions of the X-ray diffraction pattern.The vibrational motions of $FePO_4.2H_2O$ may be divided into two parts in this range: the stretching and bending vibrations of water molecules identified, respectively, around 3400 and 1610 $cm^{-1}$and the internal vibrations of $FePO_4$ located in the range (1200–400) cm^{-1}[28].

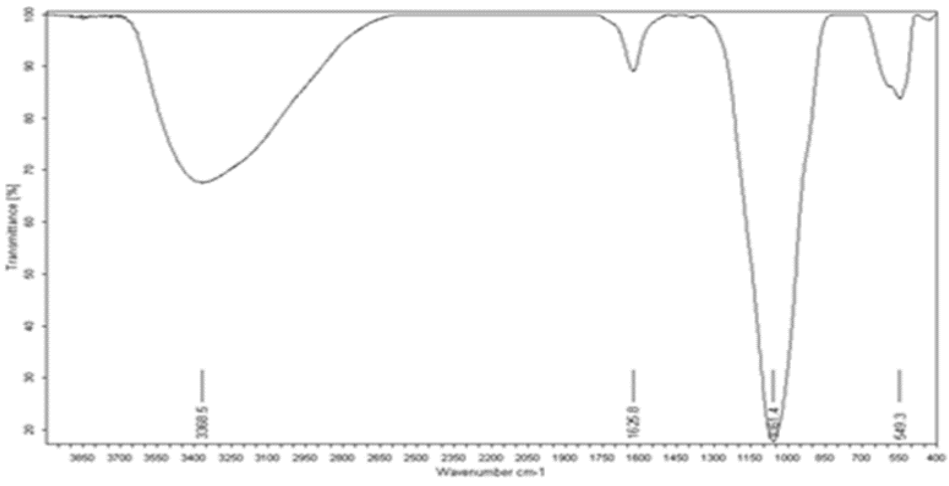

Figure11: *The FTIR spectra of $FePO_4$ $2H_2O$*

Finally, X-ray diffraction and IR spectra are in complete agreement. They indicate that it is possible to obtain a deposit of pure orthorhombic $FePO_4.2H_2O$ by electrodeposition process of a solution comprising 0.2 M of iron sulfate ($FeSO_4$) in phosphoric acid (H_3PO_4 1 M) at a potential E>0.3V/SCE.

Conclusion

This work presents a new way to synthesis at low temperature a high quality of crystalline orthorhombic $FePO_4.2H_2O$ by electrodeposition process of iron sulfate in phosphoric acid (1M) and using an oxidation potential E>0,3 V/SCE.

The mechanism of oxidation of iron sulfate in phosphoric acid (1M) was investigated. We were able to show that the oxidation isgoverned by diffusion process and the quasi-reversiblereaction at the interface of the electrode has been confirmed. The ion diffusion coefficient of Fe^{2+}inphosphoric medium(1M) is of the order of $3{,}35\times10^{-9}cm^2\ s^{-1}$.
The structural properties of the white deposit were investigated using serval complementary techniques.They confirm that$FePO_4.2H_2O$ with the orthorhombic structure was obtained.

Acknowledgment-This work was supported by MESRSFC (Ministère de l'Enseignement Supérieur et de la Recherche Scientifique et de la Formation des cadres - Morocco) and CNRST (Centre National pour la Recherche Scientifique et Technique - Morocco) (project PPR).

References

1. Y. Song, P.Y. Zavalij, M. Suzuki, M.S. Whittingham, *Inorg. Chem*. 41 (2002) 5778
2. H.N. Nang and, C. Calvo, *Can. J. Chemistry*. 53 (1975), 2064
3. K. Zaghib, C.M. Julien, *J. Power Sources.* 142 (2005) 279
4. D. Son, E. Kim, T.G. Kim, M. G. Kim, J. Cho and B. Park, *Appl. Phys. Lett*. 85 (2004) 5875
5. K.B. Gandrud,O.Nilsen, H.Fjellvag,*J. Power Sources.* 306 (2016) 454
6. Y. Wang, Z. Feng, D. Laul, W. Zhu, M. Provencher, M.L. Trudeau, A. Guerfi, K. Zaghib, *J. Power Sources* 374 (2018) 211
7. A.S. Andersson, B. Kalska, L. Haggstrom, J.O. Thomas, *Solid State Ionics.* 130 (2000) 41
8. C. Chen, G.B. Liu, Y. Wang , J.L. Li , H. Liu, *Electrochim. Acta.* 113 (2013) 464
9. D. Zhou, X. Qiu, F. Liang, S. Cao, Y. Yao, X. Huang, W. Ma, B. Yang, Y. Dai, *J. Ceramics International.* 43 (2017) 13254
10. M. Wang, Y. Xue, K. Zhang, Y. Zhang, *Electrochim. Acta.* 56 (2011) 4294
11. T.B. Zhang, Y.C. Lu, G.S. Luo, *CrystEngComm.* 15 (2013) 9104
12. D.Yu, J. Qian, N. Xue, D. Zhang, C. Wang, X. Guo, W. Ding, Y. Chen, *Langmuir.* 23 (2007) 382
13. X.X. Zhang, S.S. Tang, M.L. Chen, J.H. Wang, *J. Anal. At. Spectrom.* 27 (2012) 466.
14. W. Peng, L. Jiao, H. Gao, Z. Qi, Q. Wang, H. Du, Y. Si, Y. Wang, H. Yuan, *J. Power Sources* 196 (2011) 2841
15. N. Marx, L. Croguennec, D. Carlier, L. Bourgeois, P. Kubiak, EL. Cras, C. Delmas, *Chem, Mater*. 22 (2010) 1854.
16. X. Yang, S.M. Zhang, J.X. Zhang, M.Y. Xu, P. Ren, X.C. Li, I.C. Yan, *Funct. Mater. Let*. 4 (2011) 323
17. Y. Zhu, S. Tang, H. Shi, H. Hu, *Ceram. Int.* 40 (2014) 2685
18. Y. Yin, H. Zhang, P. Wu, B. Zhou, C. Cai. *Nanotechnology*.21 (2010).
19. M. El Joumani, S. Bououd, Z. El Abbassi , F. Saidi, A. Kafih, A. El Hourch, A. Guessous, *J. Mater. Environ. Sci.*8 (2017) 188
20. S. Bououd, A. El Hourch, K. El Kacemi, A. Guessous, A. Pradel, A. El Hourch, M. Ribes, *J. Solid State Sciences*13 (2011) 2090
21. D.P. Dubal, W.B. Kim, C.D.Lokhanden *J. Phys. Chem. Solids* 73 (2012) 18
22. P. Zhao, H. Liu , H. Zheng , Q. Tang ,Y. Guo. *Mater. Lett*. 123 (2014)128
23. A.Bard ,L.Faulkner ,R.Rosset, D.Bauer, *book. Paris. New York. Masson*, 1983.
24. L.Xiao-gang, H. Ke-long, L. su-qin, C. Li-quan, *J. Cent. South Univ. Technol*.14 (2007) 51
25. A.M. Baticle, F.Perdu, and P.Vennereau, *Electrochim.Acta*. 16 (1971) 901
26. K.K. Palkina, S.I. Maksimova, S.I. Chibiskova, K. Schlesinger, G. Ladig, Z. Anorg. *Allg. Chem.* 529 (1985) 89.
27. Y. Song, S. Yang, P.Y.Zavalij, M.S. Whittingham. *Mater. Res. Bull*. 37 (2002) 1249
28. C.M. Burba, R. Frech, *Spectrochimica Acta* Part A 65 (2006) 44

(2018) ; http://www.jmaterenvironsci.com